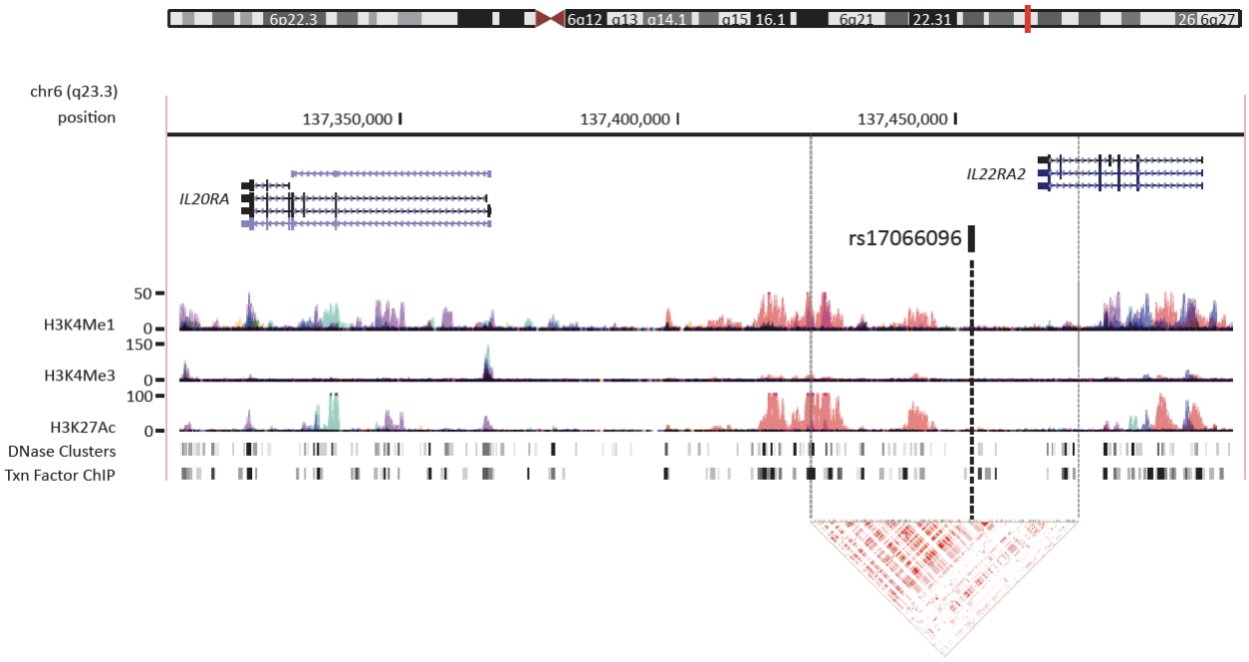

SUPPLEMENTAL FIGURE 1. MS risk locus rs17066096. Idiogram of chromosome 6 showing the location of the MS risk locus defined by the marker rs17066096. The graph displays a magnification of the locus showing the position in base pairs, nearest protein coding genes with splice variants, H3K4Me1 (often found near regulatory elements), H3K4Me3 (often found near promotors), H3K27Ac (often found near active regulatory elements, DNase I hypersensitivity clusters, and transcription factor ChIP-seq clusters, all from the ENCODE project. Image is adapted from the UCSC Genome Browser (hg19). Linkage disequilibrium (LD) plot showing R^2 values represented as a heat map in which red indicates high LD, based on 1000 Genomes phase 3 CEU population. LD plot is adapted from the Ensembl Genome Browser.

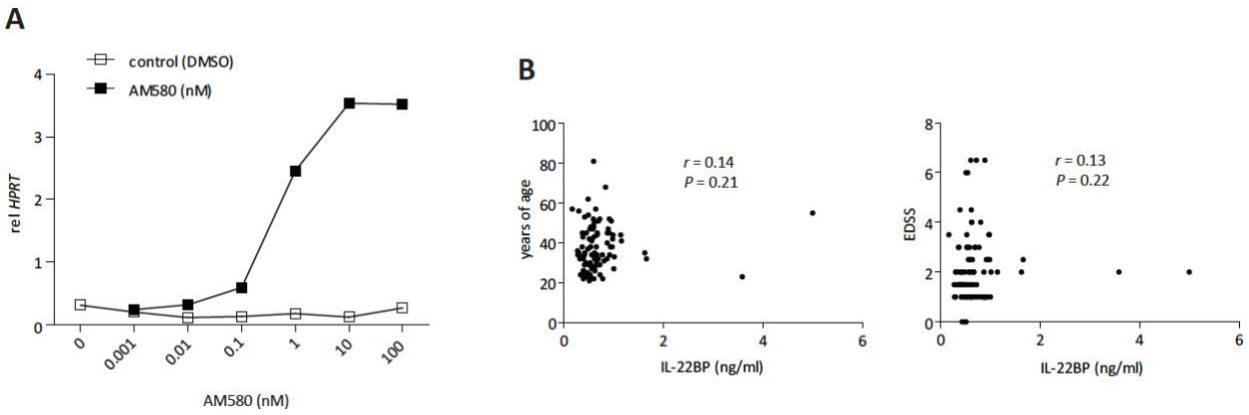

SUPPLEMENTAL FIGURE 2. AM580-*IL22RA2* dose-response curve and CSF IL-22BP vs age or EDSS. (**A**) Human peripheral blood monocytes were differentiated with GM-CSF and IL-4 for 6 days. Increasing amounts of AM580 or the same volume of vehicle (DMSO) was added from the start of the differentiation. (**B**) Human IL-22BP, determined by ELISA, in CSF from MS patients plotted against age and Expanded Disability Status Scale (EDSS). Spearman's rank correlation coefficient and two-tailed *P*-value are reported in the figure.

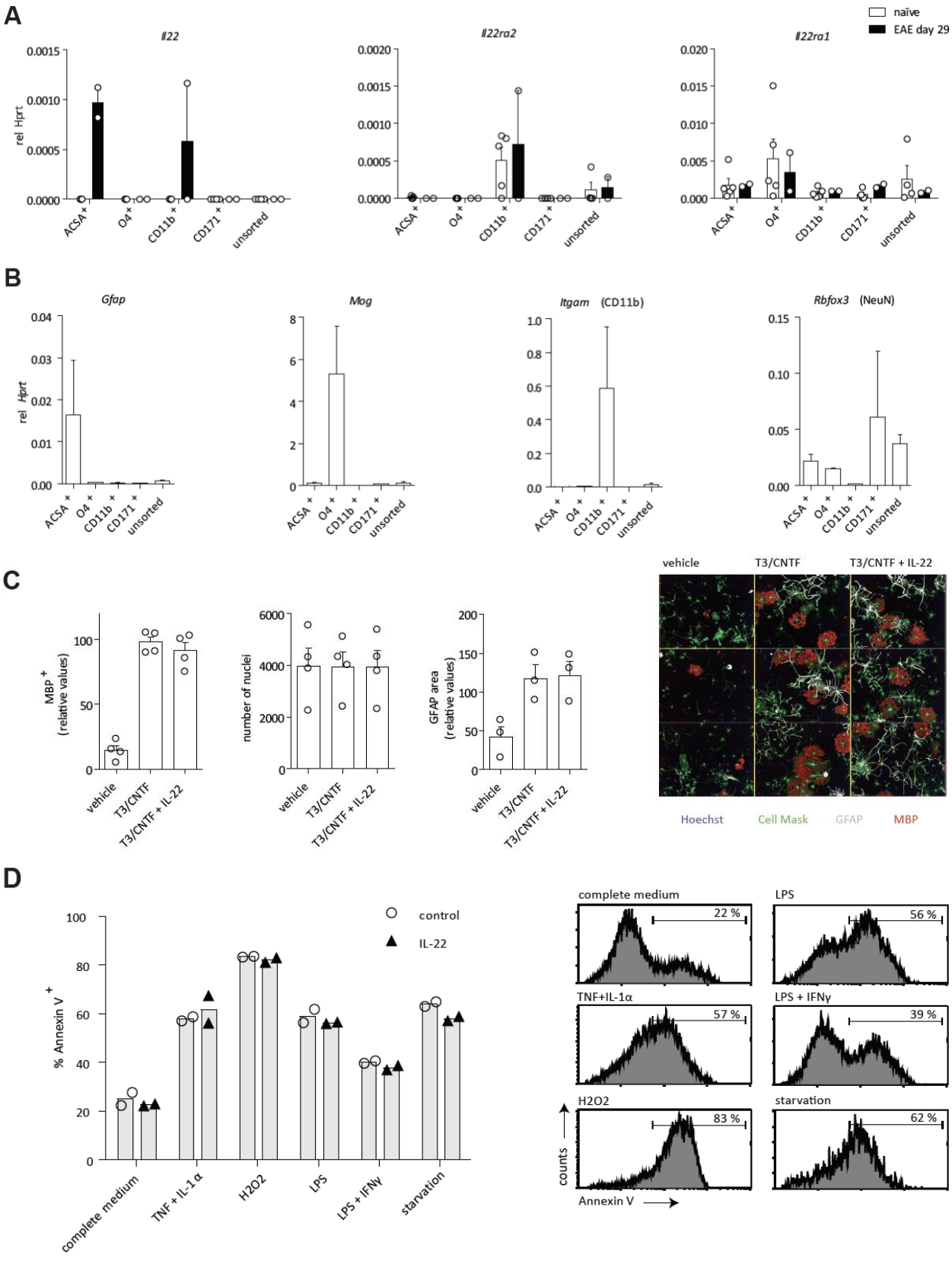

SUPPLEMENTAL FIGURE 3. The components of the IL-22-system are expressed in distinct cell populations in the mouse CNS. (**A**) Brains from naïve p2 neonatal C57BL/6 mice (*n* = 5) or adult mice taken day 29 of an EAE experiment (*n* = 2) were dissociated and the cells were enriched using magnetic beads for astrocytes (ACSA-1 and ACSA-2 combined), oligodendroglia (O4), microglia (CD11b), and neurons (CD171) followed by quantification of *Il22*, *Il22ra2*, and *Il22ra1* mRNA. (**B**) Expression of cell-type specific genes for the purpose of assessing sorting purity. (**C**) Rat oligodendrocyte precursor cells were differentiated with or without the addition of recombinant rat IL-22 in the medium. After 6 days, differentiation was assessed by quantifying cells expressing myelin basic protein (MBP) as well as overall cell number (nuclei). Presence of astrocytes could also be assessed by measuring the area with positive staining for glial fibrillary acidic protein (GFAP). Results are reported as group means +/- SEM. Representative stainings are shown. (**D**) Mouse astrocytes were isolated and cultured with a panel of conditions that induce apoptosis with or without the addition of recombinant mouse IL-22. The potential of IL-22 to influence apoptosis was examined by Annexin V-staining that was quantified using flow cytometry (*n* = 2). The histograms show representative Annexin V staining from samples without IL-22 stimulation. Results are reported as group means +/- SEM.

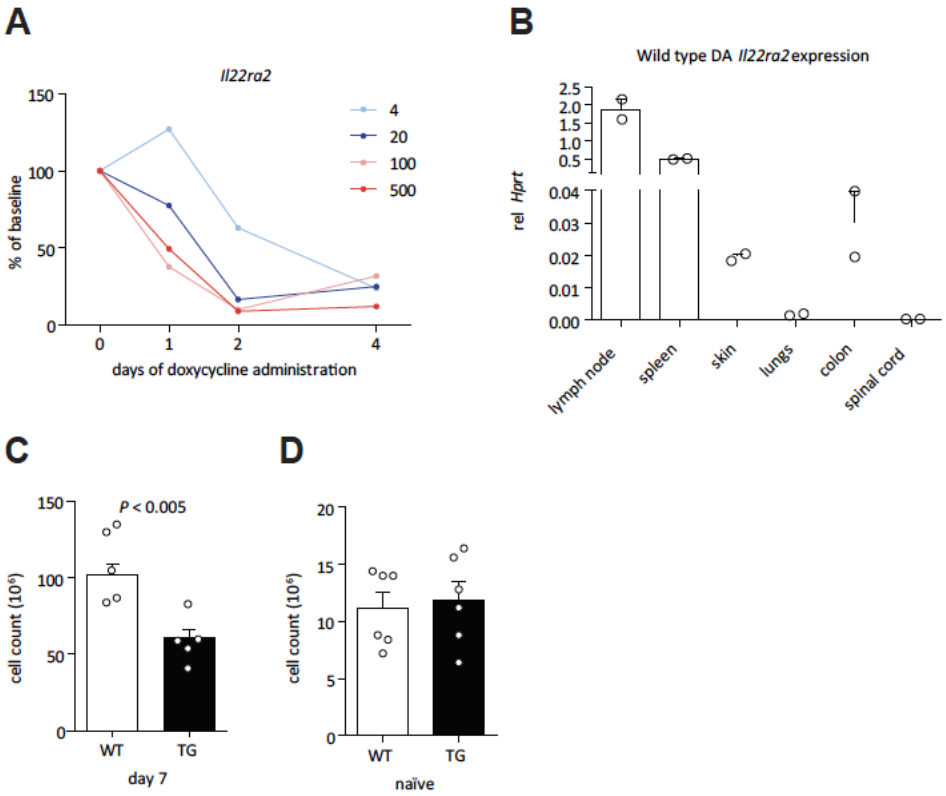

SUPPLEMENTAL FIGURE 4. Doxycycline treatment titration for rat strain with doxycycline-induced gene-specific knockdown. (**A**) Expression of *Il22ra2* in inguinal lymph nodes of rats in relation to concentration of doxycycline in the drinking water and duration of administration. Values are relative to baseline expression. Each data point represents one unique rat. (**B**) Expression of *Il22ra2* in tissue samples from naïve wild type DA rats treated with 100 mg/l of doxycycline for 10 days. The values in Fig. 3B are expressed as percentages of these. Wild type (white) and rats carrying the transgene (black) were treated with 100 mg/l of doxycycline in the drinking water for 10 days and were either (**C**) immunized with MOG after day 3 or (**D**) kept without immunization. Results are reported as group means +/- SEM and *P*-values have been calculated using two-tailed unpaired Student's *t*-test.